Resolution Effects on the Mean Square Displacement as Obtained by the Self-Distribution-Function Procedure

A Benedetto[1], S Magazù[1,*], F Migliardo[1], C Mondelli[2] and M A Gonzalez[3]

[1]Department of Physics, University of Messina, Viale Ferdinando Stagno D'Alcontres n°31, P.O. BOX 55, 98166 S. Agata, Messina, Italy
[2]CNR-INFM-OGG and CRS Soft, Institut Max Von Laue Paul Langevin, 6 rue Jules Horowitz, BP 156, F-38042 Grenoble, France
[3]Institut Max Von Laue Paul Langevin, 6 rue Jules Horowitz, BP 156, F-38042 Grenoble Cedex 9, France

E-mail: smagazu@unime.it

Abstract. In the present contribution, a procedure for molecular motion characterization based on the evaluation of the Mean Square Displacement (MSD), through the Self-Distribution Function (SDF), is presented. It is shown how MSD, which represents an important observable for the characterization of dynamical properties, can be decomposed into different partial contributions associated to system dynamical processes within a specific spatial scale. It is also shown how the SDF procedure allows us to evaluate both total MSD and partial MSDs through total and partial SDFs. As a result, total MSD is the weighed sum of partial MSDs in which the weights are obtained by the fitting procedure of *measured* Elastic Incoherent Neutron Scattering (EINS) intensity. We apply SDF procedure to data collected,by IN13, IN10 and IN4 spectrometers (Institute Laue Langevin), on aqueous mixtures of two homologous disaccharides (sucrose and trehalose) and on dry and hydrated (H_2O and D_2O) lysozyme with and without disaccharides. It emerges that the hydrogen bond imposed network of the water-trehalose mixture appears to be stronger with respect to that of the water-sucrose mixture. This result can justify the higher bioprotectant effectiveness of trehalose. Furthermore, it emerges that partial MSDs of sucrose and trehalose are equivalent in the low Q domain (0÷1.7) $Å^{-1}$ whereas they are different in the high Q domain (1.7÷4) $Å^{-1}$. This suggests that the higher structure sensitivity of sucrose should be related to the small spatial observation windows. Moreover, the role of the instrumental resolution in EINS is considered. The nature of the *dynamical transition* is highlighted and it is shown that it occurs when the system relaxation time becomes shorter than the instrumental energy time. Finally, the bioprotectants effect on protein dynamics and the amplitude of vibrations in lysozyme are presented.

1. Introduction

During the last few years, considerable efforts have been addressed, through experimental, theoretical and computational studies, to clarifying the microscopic nature of the dynamics of biological macromolecules. One of the phenomena, which has so far been widely debated, although not fully clarified, is the so-called *dynamical transition* in protein systems which, in literature, is referred to as a sharp rise in the Mean Square Displacement (MSD) of hydrated proteins compared to the dry sample, usually registered in the temperature range T=200÷240 K [1-5]. The basic understanding of the

mechanism underlying the observed *dynamical transition* remains controversial and various models have been proposed. Such a *transition* had been previously ascribed to a sudden change in an *effective elasticity* of the protein [3], to motions of specific side groups [6], to a specific fragile-to-strong crossover in dynamics of hydration water [7], to the microscopic manifestation of the glass transition in the hydration shell [8] and to a resolution effects due to a relaxation process that enters the experimentally accessible frequency window [9].

It is well known that neutron scattering allows us to characterize the structural and dynamical properties of a wide class of material systems, such as polymers and proteins. These properties can be described by the time-dependent spatial correlation function $G(\boldsymbol{r},t)$ introduced by Van Hove [10], whose space-time Fourier transform corresponds to the scattering function $S(\boldsymbol{Q},\omega)$. When the system scattering cross section is mainly incoherent, the relevant contribution is given by the self-distribution function (SDF) [10].

The experimentally obtained neutron scattering data are also connected with the employed spectrometer instrumental features. This implies that the system observables, e.g. the MSD, are influenced by instrumental effects: the energy window and the transferred wave vector values determine the time and space ranges of the observable motions. On this, several contributions are reported in literature[11-14]. In particular, Smith J C *et al*. have shown how the existence of a temperature-dependent relaxation frequency can lead to a transition in the measured MSD in the absence of any change in the Elastic Incoherent Neutron Scattering (EINS) function [13,14].

Recently, a procedure (the SDF procedure) for MSD evaluation from the EINS data has been formulated. The main aim of this work is to present the SDF procedure [15-19], to clarify how the measured intensity depends on the instrumental resolution [20-24] and to evaluate the effects of the instrumental energy resolution on the MSD extracted by EINS data [23,24].

2. Experimental Section

Experimental data were collected at the Institute Laue Langevin (Grenoble, France) using the IN4, IN13 and IN10 spectrometers. These spectrometers are characterized by a relatively high energy of incident neutrons (16 meV) and allow us to span quite a wide range of momentum transfer with three different energy resolutions.

More specifically, for the IN10 spectrometer, the incident wavelength was 6.27 Å, the Q-range was 0.30÷2.00 $Å^{-1}$ and the elastic energy resolution (FWHM) was 1 μeV, which corresponds to an elastic time resolution of 2192 ps; for the IN13 spectrometer, the incident wavelength was 2.23 Å, the Q-range was 0.28÷4.27 $Å^{-1}$ and the elastic energy resolution (FWHM) was 8 μeV, which corresponds to an elastic time resolution of 274 ps; for the IN4 spectrometer, the incident wavelength was 3.60 Å, the Q-range was 0.30÷4.5 $Å^{-1}$ and the elastic energy resolution (FWHM) was 200 μeV, which corresponds to an elastic time resolution of 11 ps.

Trehalose/19H_2O and sucrose/19H_2O mixtures and partially deuterated lysozyme in dry, D_2O, H_2O, with and without disaccharide environments at a hydration value of h=0.4 (h=g of water/g of protein) were used. The considered hydration value was chosen as the activity of proteins depends crucially on the presence of at least a minimum amount of solvent water [25,26].

Data were collected by the three spectrometers in the temperature range 20÷320 K. Empty cell contribution was subtracted and spectra were normalized to a vanadium standard. This data treatment was performed with the *Lamp* code relative to the three spectrometers used; other programs, i.e. *Mathematica*, and specific new codes were written and used for data analysis.

3. Instrumental Energy Resolution Effects on the Scattering Law

The scattering law and the intermediate scattering function are connected by a direct and an inverse time Fourier transform. The experimentally accessible quantity in the *ω-space*, due to the finite energy instrumental resolution $\Delta\omega$, is the convolution of the scattering law $S(Q,\omega)$ with the instrumental resolution function $R(\omega;\Delta\omega)$, i.e. the *measured* scattering law $S_R(Q,\omega;\Delta\omega)$.

The main aim of the present paragraph is the evaluation of the effects of the finite instrumental energy resolution. This study, which has been performed in the time domain through the time Fourier transform of the latter convolution product, yields [20-24]:

$$S_R(Q,\omega=0;\Delta\omega)=\int_{-\infty}^{\infty} I(Q,t)R(t)dt \qquad (1)$$

In the ideal elastic case in which the resolution is a delta function in the *ω-space*, we obtain from Eq. (1) that $S_R(Q,\omega=0;\Delta\omega)$ coincides with $S(Q,\omega=0)$. In figure 1, the case of IN10 and IN13 spectrometers are considered. As can be seen, two general situations can occur. The first concerns the case in which the resolution time is longer than the system characteristic time, i.e. $\tau_{RES}>\tau$, as shown in figure 1, a and b; in this circumstance, the resolution effects are relatively small; the *measured* elastic scattering laws (shadowed areas) are very close to the areas of the intermediate scattering functions. The second case occurs when the resolution time is shorter than the system characteristic time, i.e. $\tau_{RES}<\tau$, as shown in figure 1c; in this case, the resolution effects become important: the *measured* elastic scattering law is close to the area subtended by the resolution function instead of to the area of the intermediate scattering function.

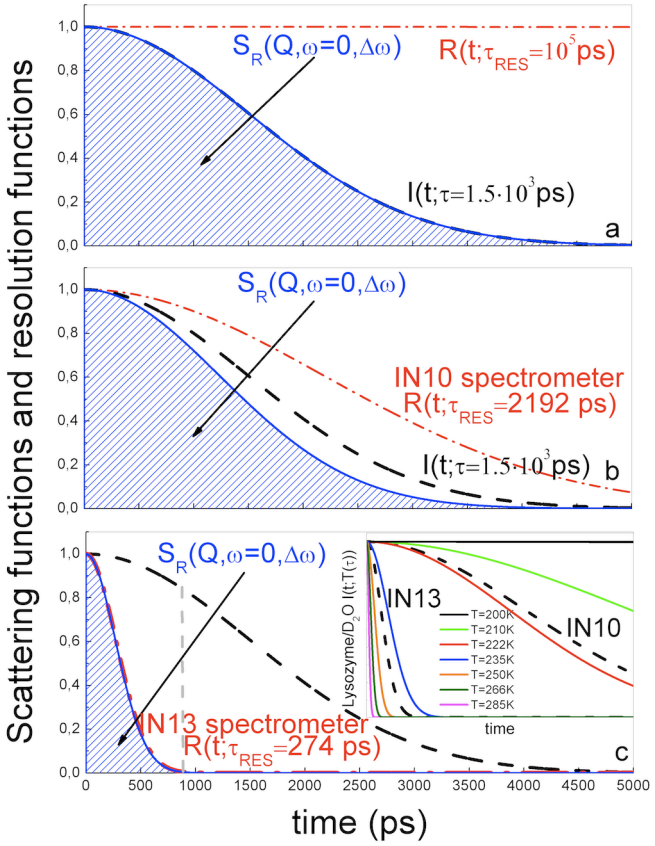

Figure 1. Resolution effects in elastic neutron scattering contribution. Comparison between the intermediate scattering function $I(t;\tau)$ at a fixed τ value (dashed curves), resolution functions $R(t;\tau_{RES})$ for different τ_{RES} values (dash-dotted curves) and the related *measured* elastic scattering laws $S_R(Q,\omega=0,\Delta\omega)$ (indicated areas). These latter, obtained considering Eq. (1), represent the *measured* elastic contribution of an elastic neutron scattering experiment on a system with a characteristic time τ in which the instrumental resolution time is τ_{RES}. (a) Case in which the resolution time is longer than the system characteristic time; no resolution effect is present: the *measured* elastic scattering law and the elastic scattering law are coincident. (b) Case in which the resolution time is slightly higher than τ:

in this case the *measured* elastic scattering law is slightly smaller than the elastic scattering law. (c) Case in which the resolution time becomes much smaller than the system characteristic time τ; the resolution effect becomes relevant: the *measured* elastic scattering law strongly differs from the elastic scattering law. (Insert) Intermediate scattering function of lysozyme/D_2O for different temperature values (data taken from Ref. [24]), and time resolution functions of IN13 and IN10 spectrometers. The intermediate scattering function crosses the resolution function at about T=220 K for IN10 and at about T=240 K for IN13.

To better understand what quantitatively happens, in figure 2 the *measured* elastic scattering law $S_R(\omega=0,\Delta\omega)$, as a function of the energy resolution, is shown. Starting from the same intermediate scattering function used for the case reported in Fig. 1 ($\tau=1.5*10^3$ *ps*), the *measured* elastic scattering law $S_R(\omega=0,\Delta\omega)$ has been evaluated as a function of the instrumental energy resolution according to Eq. (1); the areas of figure 1 have been calculated and their behaviour as a function of the instrumental energy resolution is shown. As can be seen, when $\tau_{RES}>\tau$ the resolution effects are negligible (i.e. in figure 2, the upper square, which represents the *measured* elastic scattering law corresponding to figure 1b, and the horizontal dashed-dotted line, which represents the scattering law, are close), whereas when $\tau_{RES}<\tau$ the resolution effects become important (i.e. in figure 2 the lower square, which represents the *measured* elastic scattering law corresponding to figure 1c, and the horizontal line, are far apart), and the *measured* elastic scattering law becomes equal to the area of the resolution function (dashed curve). It is important to highlight that, in the specific case reported in Fig. 1 and in Fig. 2 (i.e. Gaussian behaviour for both instrumental resolution and system scattering law functions), it can be shown that an inflexion point in the *measured* elastic scattering law occurs when the instrumental energy resolution of the used spectrometer intersects the inverse of the system relaxation time (as it can be seen in Fig. 2 considering the intersection between the vertical dashed arrow and the curve).

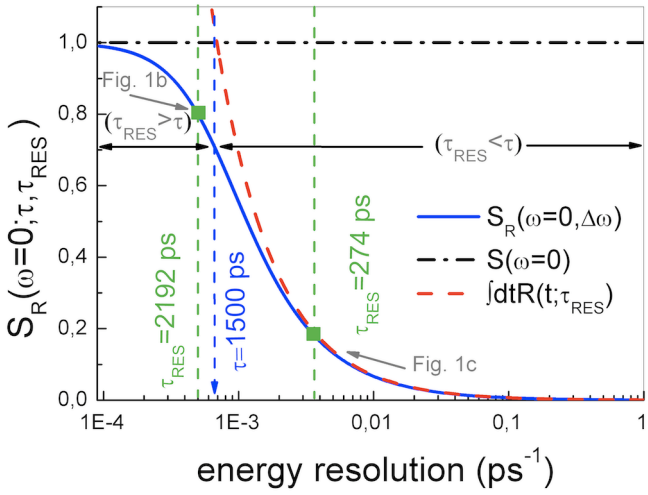

Figure 2. *Measured* elastic scattering law, $S_R(Q,\omega=0,\Delta\omega)$, as a function of energy resolution, $\Delta\omega=1/\tau_{RES}$, for system with fixed τ value. Starting from the same intermediate scattering function used for the cases reported in Fig. 1 (for which the system characteristic time is $\tau=1.5\cdot10^3$ *ps*), the $S_R(\omega=0,\Delta\omega)$ has been evaluated as a function of $\Delta\omega$ according to Eq. (1); in particular, the shadowed areas of Fig. 1 have been calculated as a function of the instrumental energy resolution and the result is here reported (full curve); the vertical dashed arrow indicates the system relaxation time. The two cases of Fig. 1 are considered (squares) and two regimes are found: when $\tau_{RES}>\tau$ the resolution effects are negligible (case of Fig. 1b); when $\tau_{RES}<\tau$, the resolution effects become important (case of Fig. 1c) and the distance between the *measured* elastic scattering law and the elastic scattering law (horizontal

dash-dotted line) increases. The change from one condition to the other one occurs when the system characteristic time intersects the resolution time; at the corresponding instrumental energy resolution value an inflection point occurs in the *measured* scattering law.

Furthermore, it is now important to take into account that the comparison between the *measured* elastic scattering laws for different instrumental energy resolutions (figure 1) is complementary to a case in which the same system is investigated at different temperature values with a fixed instrumental energy resolution (e.g. the system relaxation time obeys an Arrhenius or non-Arrhenius behaviour). To fix ideas, let us assume that by increasing temperature, the system characteristic time decreases, so giving rise to changes in the intermediate scattering function. To report a specific example, in the insert of figure 1, the behaviour of the main intermediate scattering function of hydrated lysozyme, taken at different temperature values, is reported together with the resolution function of the IN10 and IN13 spectrometers at ILL (black dashed lines). As can be seen, by increasing the temperature, the intermediate scattering function crosses the IN10 resolution function, at first, at about T=220 K and then the IN13 resolution function at about T=240 K.
Finally, in a complementary way, by applying the theorem of integral average in Eq. (1), the intermediate scattering function, evaluated at an equivalent time t^*, and $S_R(Q,\omega=0;\Delta\omega)$ are proportional [20-22]:

$$S_R(Q,\omega=0;\Delta\omega) \propto I(Q,t^*) \tag{2}$$

Now, evaluating the spatial Fourier transform of the latter equation one obtains:

$$F_r\left\{S_R(Q,\omega=0;\Delta\omega)\right\} \propto G(r,t^*) \tag{3}$$

The obtained relationship shows that, due to the fact that the SDF can be normalized, the normalized spatial Fourier Transform (F_r) of the *measured* EINS intensity profile corresponds to SDF evaluated at t^*, in which, following the standard convention for the distribution functions, r represents a displacement.

4. Self-Distribution-Function Procedure and Instrumental Energy Resolution on MSD from EINS experiments

In the following, the SDF procedure, a new procedure for MSD evaluation from EINS experiments, is presented. The SDF procedure is a recipe for MSD evaluation from EINS experiments and has been presented in previous works [15-19]. It is essentially based on the determination of the self-distribution function and on its use in the evaluation of the average statistical values of the physical quantity of interest $\langle A \rangle$, in agreement with the statistical mechanics definition:

$$\langle A \rangle = \int_{-\infty}^{\infty} A(\mathbf{r}) G^{self}(\mathbf{r})\, d\mathbf{r} \tag{4}$$

in which the spatial self-distribution function, as a probability, may be normalized to unit:

$$\int_{-\infty}^{\infty} G^{self}(\mathbf{r})\, d\mathbf{r} = 1 \tag{5}$$

In the specific case of MSD evaluation, the dynamic observable A corresponds to the second power of the displacement, $\mathbf{r}^2$:

$$\langle \mathbf{r}^2 \rangle = \int_{-\infty}^{\infty} \mathbf{r}^2 G^{self}(\mathbf{r})\, d\mathbf{r} \tag{6}$$

In the case in which the system can be considered isotropic, the volume integral becomes dependent only on the scalar r. In such a case the normalization condition and the MSD become:

$$\int_{-\infty}^{\infty} 4\pi r^2 G^{self}(r)\, dr = 1 \tag{7}$$

$$\langle \mathbf{r}^2 \rangle = \int_{-\infty}^{\infty} r^2 \left[4\pi r^2 G^{self}(r)\right] dr \tag{8}$$

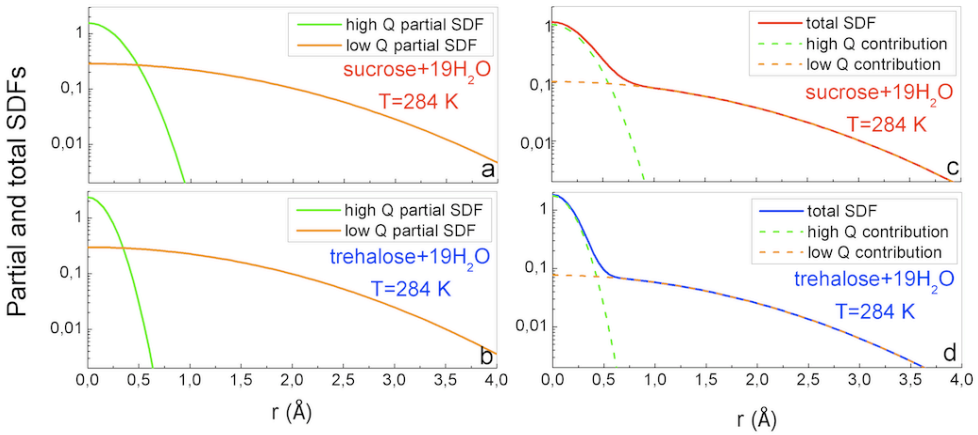

Figure 3. Partial SDFs as a function of r at T=284K for (a) sucrose/H_2O and (b) trehalose/H_2O are shown. As can be seen, the different kinds of motion are spatially well separated within the accessible Q range. Total normalized SDF as a function of r at T=284K for (a) sucrose/H_2O and (b) trehalose/H_2O together with their partial contributions are also shown. The SDF very closely follows the first partial contribution in the range (0÷0.5) Å and the second one in the range (0.5÷5.0) Å.

The SDF can be applied directly to the experimentally determined EINS profiles as well as to any function capable of reproducing EINS profile behaviour; it represents an integral procedure which takes into account the global Q behaviour and by so doing, it allows us to reduce the error on the $Q \to 0$ extrapolation. Considering that the self-distribution function can be written as a sum of Gaussian functions, as reported in Ref. [15-17,21], the normalization condition gives the following result:

$$G^{self}(r) = \sum_n A_n G_n^{self}(r) = \sum_n \frac{A_n}{16(\pi a_n)^{3/2}} \exp\left(-r^2 / 4a_n\right) \tag{9}$$

in which $\sum_n A_n = 1$; in addition the MSD is:

$$\left\langle \mathbf{r}^2 \right\rangle = 6 \sum_n A_n a_n = \sum_n A_n \left\langle \mathbf{r}^2 \right\rangle_n \tag{10}$$

in which partial SDFs and partial MSDs are present. This formula highlights that the MSD corresponds to a weighted sum of the different displacement contributions present in the system. In figure 3a and 3b, the partial SDFs as a function of r at T=284 K for sucrose/H_2O and trehalose/H_2O, respectively, are also shown. It is interesting to observe that the high-Q SDFs are different from each other whereas the low-Q SDFs are equal. Figure 3c and 3d show the obtained normalized SDF and its partial contributions as a function of r at T=284K for sucrose/H_2O and trehalose/H_2O, respectively. These functions were obtained by the fit procedure of the measured scattering intensity with Eq. (10). As can be seen, different kinds of motion are spatially well separated within the accessible Q range; furthermore, the SDF very closely follows the first partial SDF in the range (0÷0.5) Å and the second one in the range (0.5÷5.0) Å.

$\left\langle \mathbf{r}^2 \right\rangle$ represents the MSD in 3D space; if $\left\langle r^2 \right\rangle$ represents the MSD in 1D space, for isotropic systems we have that:

$$\left\langle r^2 \right\rangle = 1/3 \left\langle \mathbf{r}^2 \right\rangle \tag{11}$$

This implies that Eq. (10) in 1D yields:

$$\left\langle r^2 \right\rangle = 2 \sum_n A_n a_n = \sum_n A_n \left\langle r^2 \right\rangle_n \tag{12}$$

Therefore, this procedure allows us to obtain the autocorrelation function $G_{self}(r,t^*)$ versus r, together with its different partial contributions, as well as to determine the partial MSDs, their weights and the total MSD.

Figure 4a shows the MSD for sucrose and trehalose. Figures 4b and 4c show the partial MSDs for sucrose and trehalose, evaluated by the SDF procedure, in the temperature range 20÷287K related to the *small-r* domain and the *high-r* domain, respectively. As can be seen, the partial MSD behaviours of sucrose and trehalose are equivalent in the *high-r* domain, whereas they are different in the *small-r* domain. This circumstance suggests that the higher structure sensitivity of sucrose compared to trehalose should be related to the small spatial observation window. This finding is in agreement with several findings on disaccharide systems [27-32], in particular with inelastic neutron scattering results on the relaxation versus vibration contribution analysis, i.e. the boson peak, indicating the presence of a higher suppression of the local fast dynamics in the trehalose/water system compared to the sucrose/water system. In particular, such dynamic suppression correlates with a weaker temperature dependence of viscosity namely with a lower fragility character, which justified the higher bio-protectant effectiveness of trehalose compare to sucrose [31].

Furthermore, this finding is in agreement with other experimental findings obtained by inelastic neutron scattering which reveal a higher downshift of the OH intramolecular stretching contribution for the trehalose/water system, indicating a stronger hydrogen bonded network in the trehalose/water system compared to the sucrose/water system [32].

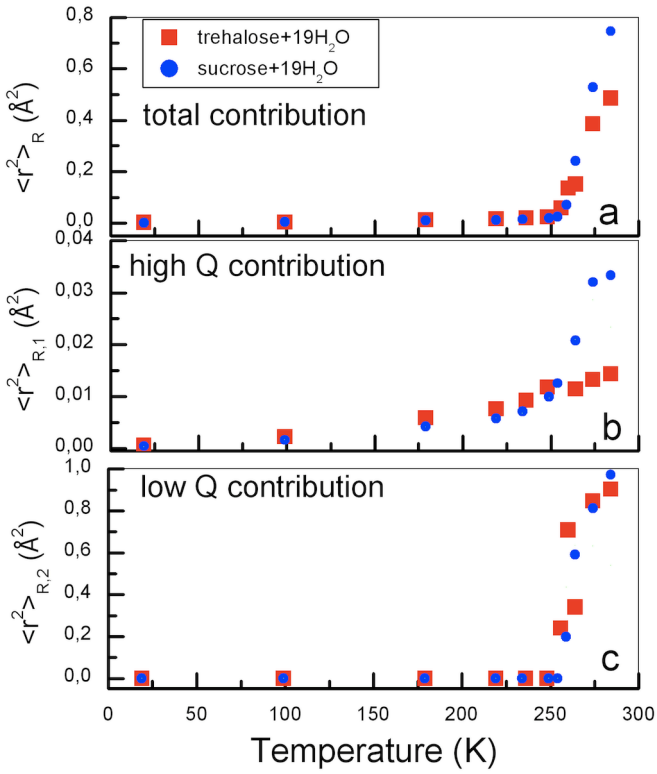

Figure 4. MSD, high Q partial MSD and low Q partial MSD temperature behaviour for trehalose/H_2O and sucrose/H_2O in the temperature range 20÷287K. As can be seen, the partial MSD behaviours of sucrose/H_2O and trehalose/H_2O are equivalent in the *high-r* domain, whereas they are different in the *small-r* domain.

To adapt the previous definition of the MSD to the case of the EINS experiments, it is necessary to consider that the instrumental energy resolution influences the physical observables as discussed in the previous paragraph; therefore Eq. (6) can be re-written as follows:

$$\left\langle r^2 \right\rangle_R = \int_{-\infty}^{\infty} r^2 G_R^{self}(r)\,dr \tag{13}$$

Starting from this relationship, in the following, we shall analyse the instrumental energy resolution effects on the MSD, in the framework of an EINS experiment. In this framework, as the output of an EINS experiment is the *measured* elastic scattering law, we have that:

$$\left\langle r^2 \right\rangle_R = \int_{-\infty}^{\infty} FT_r\left\{S_R(Q,\omega=0)\right\} r^2\,dr \tag{14}$$

where FT_r represents the spatial Fourier transform operator. For the evaluation of the MSD, let us consider Eq. (1); then Eq. (14) becomes:

$$\begin{aligned}\left\langle r^2 \right\rangle_R &= \int_{-\infty}^{\infty} FT_r\left\{S_R(Q,\omega=0)\right\} r^2\,dr \\ &= \int_{-\infty}^{\infty} FT_r\left\{\int_{-\infty}^{\infty} I(Q,t)R(t)\,dt\right\} r^2\,dr = \int_{-\infty}^{\infty}\left\{\int_{-\infty}^{\infty} G^{self}(r,t)R(t)\,dt\right\} r^2\,dr \\ &= \int_{-\infty}^{\infty} R(t)\left\{\int_{-\infty}^{\infty} G^{self}(r,t) r^2\,dr\right\} dt = \int_{-\infty}^{\infty}\left\langle r^2\right\rangle(t)R(t)\,dt\end{aligned} \tag{15}$$

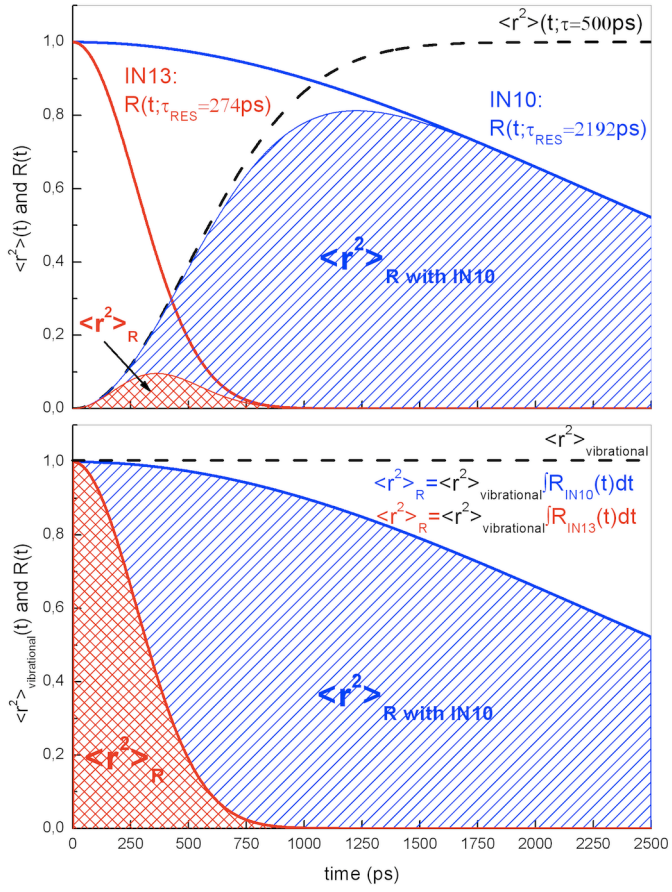

Figure 5. (a) Normalized time behaviour of the actual "system MSD" at a fixed τ value, $\langle r^2\rangle(t;\tau)$ (dashed curve); resolution function for different τ_{RES} values (curves), $R(t;\tau_{IN13})$ and $R(t;\tau_{IN10})$; *measured* MSD $\langle r^2\rangle_R$ evaluated by Eq. (15). (b) Effect on the *measured* MSD due to the different energy

resolution of the two spectrometers, IN13 and IN10, when only vibrational motions occur; in particular, as can be seen, different *measured* MSDs correspond to the same actual system MSD.

More specifically, $\langle r^2 \rangle(t)$ is the actual "system MSD", while $\langle r^2 \rangle_R$ is the "*measured* MSD". The first is a function of time, whereas the second is the MSD value as obtained by EINS; it is a pure number, not a function of time, and depends on the instrumental resolution used. Figure 5a shows the effect on the *measured* MSD due to the resolution function used: due to the different energy resolutions used different *measured* MSDs correspond to the same actual system MSD.
Finally, it is interesting to observe what occurs in the vibrational motions domain, e.g. at low temperature value. When only vibrational motions occur, the actual system MSD can be considered almost constant $\langle r^2 \rangle(t) \rightarrow \langle r^2 \rangle^{(V)}$ (such a condition is approximately satisfied in the low temperature range up to T=40 K); in such a case, the *measured* MSD from Eq. (15) is:

$$\langle r^2 \rangle_R = \int_{-\infty}^{\infty} \langle r^2 \rangle(t) R(t)\, dt = \int_{-\infty}^{\infty} \langle r^2 \rangle^{(V)} R(t)\, dt = \langle r^2 \rangle^{(V)} \int_{-\infty}^{\infty} R(t)\, dt \qquad (16)$$

Then, starting from Eq. (16), it is possible to determine the actual system MSD at the lowest temperature values. Figure 5b shows the effect on the *measured* MSD due to the use of a different energy resolution; as can be seen, different *measured* MSDs correspond to the same actual system MSD. A validity test of the proposed procedure is obtained by applying this procedure to the data collected on the same systems, i.e. dry and hydrated lysozyme (see the insert of figure 6), by the two spectrometers IN13 and IN10, working at a different energy resolution. As a result, at the lowest temperature values we obtain the same actual system mean displacement values, i.e. 0.016 Å [23].
It is also of interest to examine the normalization procedures most frequently applied both on the measured elastic scattered intensity, and on the extracted MSD.
It is well known that the *measured* scattering law, which is a function of Q, represents the number of elastically diffused neutrons within a given solid angle. Therefore, normalization consisting in a multiplicative factorization, i.e. $S_R \rightarrow nS_R$, is an allowed transformation able to rescale the data since it does not change the proportionality relationship between the scattering intensity at different Q values. This transformation may be useful, for example, to give the same intensity value (e.g. at the origin) to different spectra collected at different temperatures and does not produce any change in MSD evaluation.
In this regard, it should be taken into account that, on the contrary, the same kind of normalization applied to the logarithm of the *measured* scattering law is a misleading procedure since it leads to an incorrect evaluation of the MSD value. In fact, the normalization of the logarithm of the *measured* scattering law corresponds to a power elevation of the *measured* scattering law, i.e. $nLn(S_R) \rightarrow (S_R)^n$, which gives an incorrect MSD, i.e. $n\langle r^2 \rangle_R$.
On the other hand, as far as the logarithm of the *measured* scattering law is concerned, it can be observed that the proper transformation is a translation, this latter corresponding to a normalization of the *measured* scattering law: $Ln(S_R) + Ln(n) \rightarrow nS_R$.
Finally, the normalization of the *measured* scattering law for the *measured* scattering law obtained at a given temperature (usually the lowest) is again wrong since it changes the relationship between the *measured* scattering law relative to different Q values; this procedure would bring a shift of the MSD, assigning it the value of zero at the lowest temperature: $S_R(T) / S_R(T_0) \rightarrow MSD = \langle r^2 \rangle_R(T) - \langle r^2 \rangle_R(T_0)$.
Regarding this, it is worth observing that the method previously described for obtaining the vibrational MSD value, which is based on the instrumental energy resolution effects evaluation, clarifies how a correct normalization of both the scattering functions and the MSD trends should be performed.

5. Protein *Dynamical Transition*

In the third paragraph, addressed to the description of the instrumental energy resolution effect in EINS, it is highlighted that an inflection point in the *measured* scattering law occurs when the system relaxation time intersects the instrumental energy resolution time. This finding also implies that sometimes, transitions in the *measured* elastic scattering laws may have mistakenly been attributed to real transitions in the dynamic properties of the systems, instead of the simple instrumental effect. More specifically, because a transition in the *measured* elastic scattering law as a function of temperature generates a transition in the extracted MSD temperature behaviour, also transitions in the MSDs may have been mistakenly attributed to real transitions in the dynamic properties of the systems instead of the simple instrumental resolution effect. As highlighted by Smith J C *et al*. [13,14] and by Sokolov A P *et al*. [9], this may be the case of the so-called *dynamical transition*, which represents an open question in the biophysical field. In particular, Sokolov A P *et al*. in Ref. [9] by combining neutron and dielectric spectroscopy data, have shown that there is no sudden change in the dynamics of the protein at temperatures around 200÷230 K, and, therefore, these authors have proposed that the *dynamical transition* is just a result of the protein's structural relaxation reaching the limit of the experimental frequency window.

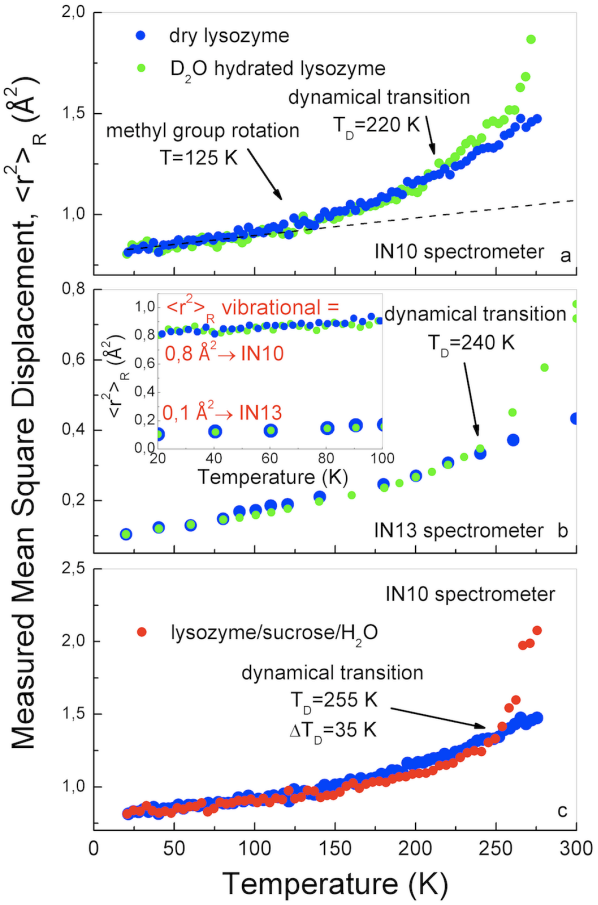

Figure 6. *Measured* MSDs of lysozyme obtained using two different spectrometers with two different instrumental energy resolutions. Comparison between the *measured* MSD temperature behaviour of dry and D_2O hydrated lysozyme, obtained from data collected by both (a) IN10 and (b) IN13 spectrometers. The *dynamical transition* temperature is T_D=220 K from IN10 data and T_D=240 K from IN13 data. (c) Comparison between the *measured* MSDs obtained for H_2O hydrated lysozyme with sucrose and dry lysozyme by the IN10 spectrometer. The presence of disaccharide shifts the *dynamical transition* to a higher temperature value of T=255 K. (Insert) Comparison between the dry

and D_2O hydrated lysozyme *measured* MSDs both from IN10 and IN13 spectrometers in the low temperature range when only vibrational motions occur. The *measured* MSD is about 0.8 $Å^2$ with IN10 and about 0.1 $Å^2$ with IN13. This discrepancy is connected to resolution effects and can be used to determine the system vibrational motion amplitudes.

More specifically, with regard to hydrated lysozyme samples, it has recently [24] been demonstrated that the so-called *dynamical transition*: (i) is a finite instrumental energy resolution effect, and, more specifically, appears when the characteristic system relaxation time intersects the resolution time, (ii) it does not imply any transition in the dynamical properties of systems, (iii) it is not due to the fragile-to-strong- dynamical crossover (FSC) in the temperature behaviour of the system relaxation time, differently to what Chen S H et al. proposed in Ref. [7].
In figure 6, the average *measured* MSDs as a function of temperature are shown for dry and hydrated lysozyme, with and without sucrose, evaluated by the SDF procedure in the range 20÷287 K. The MSDs are obtained using two different instrumental energy resolutions. The *dynamical transition* temperature is T_D=220 K from IN10 data, in which the resolution used is 1 μeV, and T_D=240 K from IN13 data, in which the resolution used is 8 μeV. These values are in agreement with the conclusion on the nature of the *dynamical transition* presented in Ref. [24]. In fact, as can be seen in the temperature behaviour of the system relaxation time [24], a relaxation time of τ=2192 ps corresponds to the temperature value of T=220 K, which is equal to the *dynamical transition* temperature value obtained with IN10 for which the instrumental resolution time is τ_{RES}=2191 ps; moreover, a relaxation time of τ=274 ps corresponds to the temperature value of T=240 K, which is equal to the *dynamical transition* temperature value obtained with IN13 for which the instrumental resolution time is τ_{RES}=274 ps.
Finally, a confirmation of this finding can be given considering that the presence of disaccharides shifts the system relaxation time towards higher values [33] and, therefore, the above *dynamical transition* must occur at the higher temperature when sucrose is added. As can be seen in Fig. 6c, the presence of disaccharide shifts the *dynamical transition* to a higher temperature value of T=255 K.

6. Conclusion

In this paper, a general presentation of the SDF procedure applied on two homologous disaccharides, i.e. sucrose and trehalose, was presented; the energy resolution effects on neutron scattering functions were also discussed.
The SDF procedure was presented for the first time in Ref. [15], then, in Ref. [16] it was theoretically improved and applied on polyethylene glycol with a mean molecular weight of 400 Dalton. An experimental check of the procedure was also performed in Ref. [16] by its application on hydrogenated and on two partially deuterated polyisoprene systems. In Ref. [17], the procedure was also improved and was applied to dry myoglobin in a trehalose matrix. Then, the effects of the instrumental energy resolution on the scattering functions was taken into account in Ref. [20].
The case of the two homologous disaccharides (trehalose and sucrose), which is partially discussed in the present paper, was treated in Ref. [19,21,22] within a comparison between the SDF procedure and the common Gaussian protocol for the MSD determination. For the first time, the higher mobility of sucrose/H_2O compared to trehalose/H_2O was related to a specific spatial domain. In particular, in Ref. [19] the effects of natural bioprotectants on the protein *dynamical transition* are shown. Then the effects of the instrumental energy resolution directly on the measured MSD were computed and presented in Ref. [23].
In the light of the obtained results, a complete analysis of the neutron scattering spectra has allowed us to solve the puzzling question of the so-called *dynamical transition*. In Ref. [23,24], the idea that the *dynamical transition* was due to the fact that the system characteristic time crosses the time corresponding to the finite energy resolution was presented. This idea was connected to the fact that the *dynamical transition* temperature obtained using different instrumental energy resolutions

coincides case by case with the temperature for which the system relaxation time and the resolution time are equal (compare the *dynamical transition* temperature of figure 6 with the relaxation time reported in Ref. [7,9]). In the same paper [23], the determination of the amplitude of vibration motion in dry and hydrated (H_2O and D_2O) lysozyme was also shown.

7. References

[1] Doster W, Cusak S and Petry W 1989 *Nature* **337** 754
[2] Rasmussen B F, Stock A M, Ringe D and Petsko G A 1992 *Nature* **357** 423
[3] Zaccai G 2000 *Science* **288** 1604
[4] Doster W 2008 *Eur. Biophys. J.* **37** 591
[5] Sokolov A P, Roh J H, Mamontov E and Garcia Sakai V 2008 *Chem. Phys.* **345** 212
[6] Lee A L and Wand J 2001 *Nature* **411** 501
[7] Chen S H, Liu L, Fratini E, Baglioni P, Faraone A and Mamontov E 2006 *Proc. Natl. Acad. Sci. U.S.A.* **103** 9012
[8] Doster W, Busch S, Gasper A M, Appavou M S, Wuttke J and Scheer H 2010 *Phys. Rev. Lett.* **104** 098101
[9] Khodadadi S, Pawlus S, Roh J H, Garcia Sakai V, Mamontov E and Sokolov A P 2008 *J. Chem. Phys.* **128** 195106
[10] Van Hove L 1954 *Phys. Rev.* **95** 249
[11] Gabel F and Bellissent-Funel M C 2007 *Biophys. J.* **92** 4054
[12] Kneller G R and Calandrini V 2007 *J. Chem. Phys.* **126** 125107
[13] Becker T and Smith J C 2003 *Phys. Rev. E* **67** 021904
[14] Becker T, Hayward J A, Finney J L, Daniel R M and Smith J C 2004 *Biophys. J.* **87** 1436
[15] Magazù S, Maisano G, Migliardo F and Benedetto A 2008 *J. Molec. Struct.* **882** 140
[16] Magazù S, Maisano G, Migliardo F and Benedetto A 2008 *Phys. Rev. E* **77** 061802
[17] Magazù S, Maisano G, Migliardo F and Benedetto A 2008 *J. Phys. Chem. B* **112** 8936
[18] Magazù S, Migliardo F, Benedetto A, Gonzalez M and Mondelli C 2010 *Spectroscopy* **24** 387
[19] Magazù S, Migliardo F, Benedetto A, Mondelli C and Gonzalez M 2011 *J. Non Cryst. Sol.* **357** 664
[20] Magazù S, Maisano G, Migliardo F, Galli G, Benedetto A, Morineau D, Affouard F and Descamps M 2008 *J. Chem. Phys.* **129** 155103
[21] Magazù S, Maisano G, Migliardo F and Benedetto A 2009 *Phys. Rev. E* **79** 041915
[22] Magazù S, Maisano G, Migliardo F and Benedetto A 2010 *Biochim. et Biophys. Acta* **1804** 49
[23] Magazù S, Migliardo F and Benedetto A 2010 *J. Phys. Chem. B* **114** 9268
[24] Magazù S, Migliardo F and Benedetto A 2011 *J. Phys. Chem. B* **115** 7736
[25] Careri G 1998 *Prog. Biophys. Mol. Biol.* **70** 223
[26] Gregory R B 1995 *Protein-Solvent Interactions* Dekker, New York
[27] Ballone P, Marchi M, Branca C and Magazú S 2000 *J. Phys. Chem. B* **104** 9268
[28] Branca C, Magazù S, Maisano G and Migliardo F 2001 *Phys. Rev. B* **64** 224204
[29] Affouard F, Bordat P, Descamps M, Lerbret A, Magazù S, Migliardo F, Ramirez-Cuesta A J and Telling M F T 2005 *Chem. Phys.* **317** 258
[30] Magazù S, Maisano G, Migliardo P and Villari V 1999 *J. Chem. Phys.* **111** 9086
[31] Magazù S, Migliardo F, Affouard F, Descamps M and Telling T F 2010 *J. Chem. Phys.* **132** 184512
[32] Branca C, Magazù S, Maisano G, Bennington S M and Fak B 2003 *J. Phys. Chem. B* **107** 1444
[33] Lerbret A, Bordat P, Affouard F, Hedoux A, Guinet Y and Descamps M 2007 *J. Phys. Chem. B* **111** 9410

Acknowledgments

The authors wish to acknowledge the Institut Laue-Langevin (ILL), Grenoble, France for beam time on IN4, IN10 and IN13 spectrometers.